



METHOD

# Long-term Fiber Photometry for Neuroscience Studies

Yi Li<sup>1</sup> · Zhixiang Liu<sup>1</sup> · Qingchun Guo<sup>2</sup> · Minmin Luo<sup>1,3</sup>

Received: 21 November 2018 / Accepted: 25 February 2019 / Published online: 6 May 2019  
© Shanghai Institutes for Biological Sciences, CAS 2019

**Abstract** Fiber photometry is a sensitive and easy way to detect changes in fluorescent signals. The combination of fiber photometry with various fluorescent biomarkers has substantially advanced neuroscience research over the last decade. Despite the wide use of fiber photometry in biomedical fields, the lack of a detailed and comprehensive protocol has limited progress and sometimes complicated the interpretation of data. Here, we describe detailed procedures of fiber photometry for the long-term monitoring of neuronal activity in freely-behaving animals, including surgery, apparatus setup, data collection, and analysis.

**Keywords** Ca<sup>2+</sup> signal · Fluorescence detection · Ca<sup>2+</sup> indicator · Optical fiber · Experiment protocol

## Introduction

Fiber photometry is widely used to monitor neuronal activity in freely-behaving animals in modern experimental neuroscience research [1–13]. Fiber photometry techniques for neuroscience employ an optical fiber implanted into the brain to enable study of the function of specific populations of neurons. Briefly, excitation light of a specific wavelength

is delivered through the fiber and this excites a fluorescent probe to generate fluorescence. Subsequently, the fluorescence signal in the immediate vicinity of the distal end of the fiber is returned *via* the same fiber, reaching a sensitive photodetector that converts the information about fluorescence intensity into an analog signal. Finally, software is used to record the digitized intensity of the detected fluorescence signal. Understanding the basic principles of fiber photometry allows immediate experimental adjustments and full customization as necessary. The following protocols are based on the techniques that we use in our laboratory for long-term fiber photometry recording.

## Advantages and Limitations

By combining fluorescent reporters with fiber photometry, researchers can monitor the activity of cell-type-specific neurons [1–13] and even the expression levels of specific genes [14]. Monitoring the activity of neurons and searching for correlations between neuronal activity and natural animal behavior is a fundamentally important experimental strategy for studying the functions of the brain. Traditional electrophysiological recording with high temporal resolution has been widely used [15] and has revealed vast insights with large implications that have deepened our understanding of neural circuit functions. By expressing light-sensitive proteins, electrophysiological recordings with optical tagging have enabled researchers to record the activity of cell-type-specific neurons [16, 17]. However, electrophysiological recording with “optical tagging” is technically challenging, is sensitive to noise interference in many natural behaviors, and is not efficient.

By taking advantage of genetically-encoded Ca<sup>2+</sup> indicators such as GCaMP proteins [18], fiber photometry is able to monitor the activity of genetically-defined neuron

✉ Minmin Luo  
luominmin@nibs.ac.cn

<sup>1</sup> National Institute of Biological Sciences, Beijing 102206, China

<sup>2</sup> Thinker Tech Nanjing Biotech Limited Co., Nanjing 210019, China

<sup>3</sup> School of Life Sciences, Tsinghua University, Beijing 100084, China

populations. Using fiber photometry, numerous groups have made exciting observations of neuronal activation patterns during affective reward- and punishment-related behaviors [9, 11, 12], feeding behaviors [4], social behaviors [6, 9, 11], arousal [7, 10], and long-term learning [11, 12]. Fiber photometry also enables the measurement of gene expression levels. Recently, fiber photometry has been used in a study of circadian rhythms by monitoring circadian clock gene expression using bioluminescent reporters [14]. Although fiber photometry is currently relatively poor in temporal and spatial resolution compared to traditional electrophysiological recording techniques, it is easier to use, much more resistant to electrical interference, more efficient for data collection, more stable for long-term monitoring, and considerably less expensive.

## Materials and Methods

### Animals

Before surgery, mice were maintained under a 12/12 h light/dark cycle and housed in groups. After surgery, they were either housed in groups or individually for at least one week for recovery before further experiments. Animals of either sex were used for fiber photometry recording. Animal care and use conformed to both the institutional guidelines of the National Institute of Biological Sciences and governmental regulations (Approval ID: NIB-SLuoM15C). Note that although the techniques described in this protocol were optimized for use in rodents, they are readily adaptable for use in other animal species.

### Viral Vectors

We used the genetically-encoded  $\text{Ca}^{2+}$  indicator GCaMP6m to monitor the activity of neurons. Other indicators that have comparable sensitivity and signal-to-noise ratios are also applicable for photometry recording [1, 18]. mGFP-expressing animals were used as controls for comparison with GCaMP6m-expressing animals. We packaged our own Cre-recombinase-dependent AAV vectors as described [15]. AAV vectors carrying DIO-mGFP or DIO-GCaMP6m constructs were packaged into the AAV2/9 serotype, with titers of  $1 \times 10^{12}$ – $5 \times 10^{12}$  viral particles/mL; these viral vectors can be purchased from many commercial companies (*e.g.*, Taitool, Shanghai; BrainVTA, Wuhan; Vigenebio, Jinan, China) or from non-profit organizations such as the University of North Carolina, the University of Pennsylvania, and Stanford University, and Addgene (Watertown, MA, USA). Note that the present protocol report does not detail procedures

for packaging AAV viral vectors. We injected the virus as described previously [19].

### Materials for Optical Fiber Construction

The type of optical fibers used for fiber photometry are similar to those for optogenetic experiments. We constructed implantable fibers in our lab mainly as described previously [20], but with some modifications specific for fiber photometry recordings. This protocol details the construction of implantable fibers using LC/SC-sized ceramic fiber ferrules with a 230- $\mu\text{m}$  inner diameter and 200- $\mu\text{m}$  multimode optical fibers with a numerical aperture (NA) of 0.37 or higher. Similar devices are commercially available, for example the fiber optic cannula systems offered by Thinker Tech (Nanjing, China), RWD Life Science (Shenzhen, China), Thorlabs (Newton, NJ, USA), and Doric Lenses (Quebec, Quebec, Canada). However, these systems may not be fully customizable to meet the specific requirements for all types of fiber photometry experiments. The procedures for optical fiber construction are also included in this protocol.

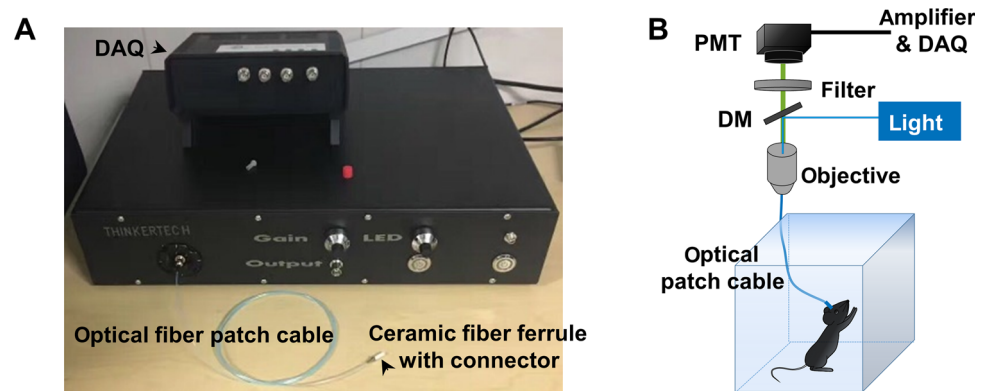
### Equipment for Fiber Photometry Recording

Various types of fiber photometry system are available commercially [21–23], all of which are based on a similar fluorescence detection scheme. We used a single-channel fiber photometry system (Fig. 1A, Thinker Tech). To record fluorescence signals, the beam from a 488-nm laser or filtered light-emitting diode (LED) is reflected by a dichroic mirror, focused by a 20 $\times$  objective lens, and then coupled to a fiber patch cable (Fig. 1B), which guides the light between the objective and the implanted optical fiber (Fig. 1B). The GCaMP fluorescence is collected by the same fiber and objective, then bandpass-filtered and detected by a photomultiplier tube (PMT). An amplifier converts the PMT current output to a voltage signal, which is further filtered through a low-pass filter (40 Hz cut-off). The analog voltage signal is finally acquired at 100 Hz–200 Hz, using customized software routines developed in MatLab (Natick, MA, USA) or LabVIEW (Austin, TX, USA).

### Quality Control

The light output of each of the optical fibers to be implanted should be measured before implantation. It is important to use fibers with high transmission efficacy for fiber photometry recording. The light transmission efficacy of such a fiber is the ratio between the light power with the fiber (1) attached to and (2) not attached to the fiber patch cable when the laser is on continuously. For any surgical

**Fig. 1** The fiber photometry system. **A** Image of a commercial single-channel fiber photometry system (courtesy of Nanjing Thinker Tech). DAQ, data acquisition. **B** Schematic diagram of the fiber photometry system with a behaving animal connected to the optical patch cable. PMT, photomultiplier tube; DM, dichromatic mirror.



implantation, we only use implantable optical fibers with a tested transmission efficacy > 85%.

Fluorescence signals are checked 7–10 days after surgery for each animal bearing a fiber implant. As the criterion for a successfully implanted and useable fiber, we usually use three standard deviations of the recorded signal as the threshold; that is, only animals with significant fluctuation of the fluorescent signal (greater than threshold) are used in further experiments. The position of the fiber tip and the expression of fluorescent protein should be verified for each animal after a completed experiment (examined *post mortem*).

In addition to implanting fibers into animals expressing GCaMP6m, naive or control mice only expressing genetically-encoded GFP should also be implanted to ensure that any outcomes recorded by the fiber photometry system are not caused by behavioral artifact(s).

## Reagents

Five-minute epoxy.  
 Pentobarbital (stock 50 mg/mL).  
 Tribromoethanol.  
 Erythromycin eye ointment (Shuangji Pharmacy Limited Company, Beijing, China).  
 75% ethanol, H<sub>2</sub>O<sub>2</sub>, and NaCl.  
 Dental cement (Pigeon Dental, Shanghai, China).  
 Black nail polish.  
 Lincomycin hydrochloride and lidocaine hydrochloride gel (Fangming Pharmaceutical Group Co, Ltd, Shandong, China).  
 Isoflurane (RWD Life Science, Shenzhen, China).

## Equipment

### Implantable Optical Fiber Construction

Optical fibers (200- $\mu$ m core, 0.37 NA; Thorlabs, Newton, NJ, USA).

Ceramic fiber ferrules (LC/SC type, 230- $\mu$ m inner diameter; Fiberlaser, Shanghai, China).

Ceramic connectors (LC/SC type; Fiberlaser, Shanghai, China).

Fiberoptic stripper (Ripley Tools CFS-2, Cromwell, IN).

Fiber cleaver (Gear GR-27, Zibo, Shandong, China).

Stereomicroscope (Olympus SZ61, Tokyo, Japan).

Glass coverslips (20 mm  $\times$  20 mm).

Toothpicks and cotton swabs.

### Measuring the Light Transmission Efficacy of Implantable Optical Fibers

Fiber photometry system (Thinker Tech, Nanjing, China).

Optical patch cable (FC type, 200- $\mu$ m core, 0.37 NA; Fiberlaser, Shanghai, China).

Laser power meter (Sanwa LP1, Tokyo, Japan).

### Virus Injection and Optical Fiber Implantation

Surgical tools including scissors, tweezers, and scalpel blades.

Stereotaxic apparatus (RWD Life Science or Thinker Tech).

Syringe tip from 1 mL syringe (Misawa Medical Industry Co., Ltd, Shanghai, China).

Micro-screw driver and M1 screws.

Nanoliter 2010 micro-injection pump (WPI, Sarasota, FL, USA).

Micro4 controller (WPI, Sarasota, FL).

## Procedures

### Implantable Optical Fiber Construction (Fig. 2, 1 h)

1. Cut 150 mm–200 mm of optical fiber from the spool using wire cutters.

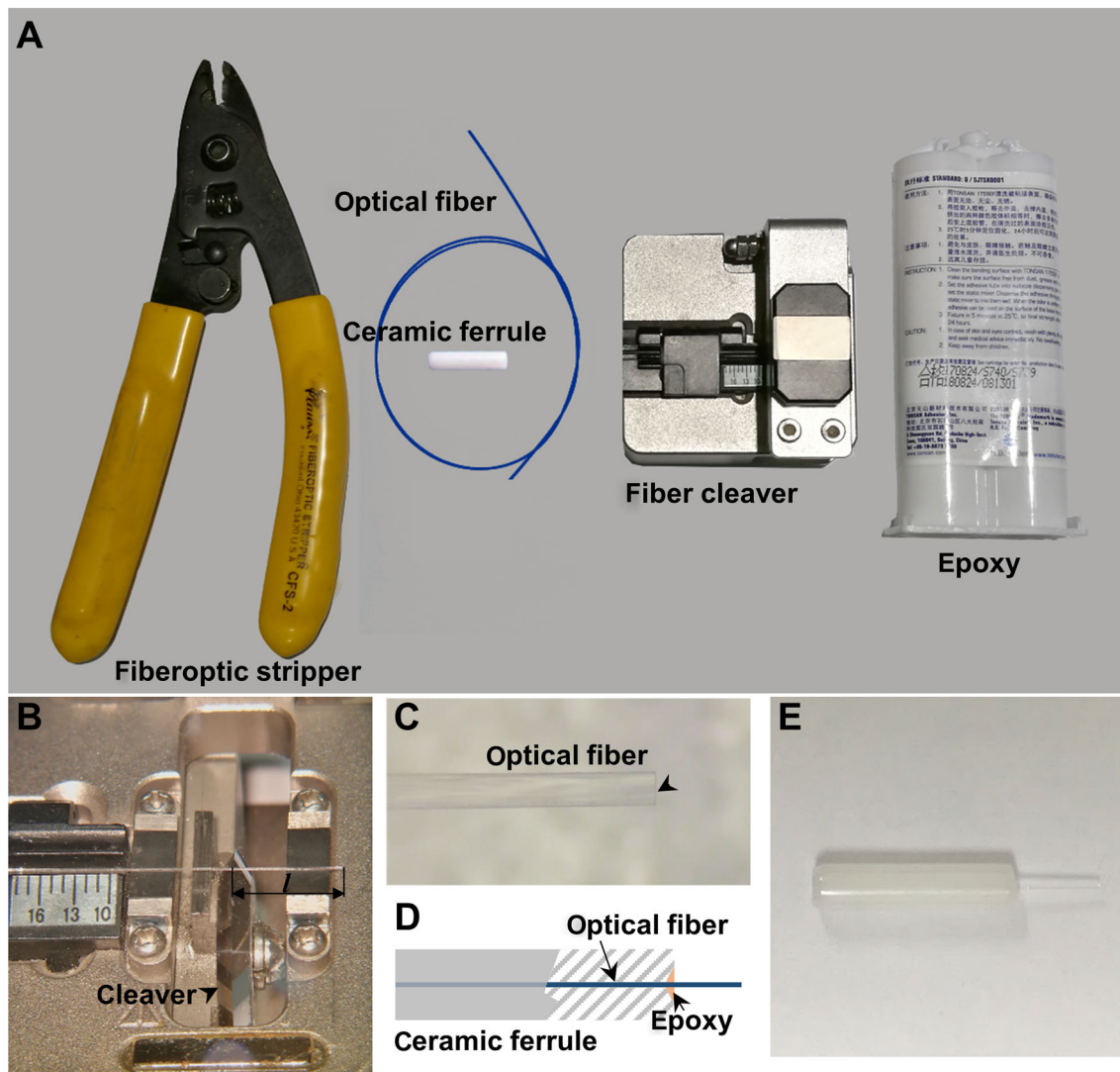


**Fig. 2** Construction of implantable optical fiber. **A** Main equipment for implantable optical fiber construction. **B** Stripped optical fiber on the fiber cleaver. *l*: optical fiber length. **C** Optical fiber with a flat end

(black arrowhead). **D** Schematic diagram of fixing an optical fiber into the ceramic ferrule with epoxy. **E** Photograph of a prepared implantable optical fiber.

**Note:** These lengths are enough to prepare 10–20 implantable fibers.

- Strip the coating off the 200- $\mu\text{m}$  core fiber using a fiber-optic stripper. Strip only 30 mm–50 mm each time.
- Put the stripped core fiber onto the fiber cleaver, adjust it to the appropriate length, hold the unstripped end tight, and move the blade of the fiber cleaver to cut it (Fig. 2B).  
**Note:** This step determines the length of the fiber, so make sure that the selected size is suitable for probing the nucleus of interest (e.g., dorsal raphe nucleus).
- Check the tip of each fiber with a stereomicroscope. Only use those with a flat tip end (Fig. 2C).

**Note:** If the tip end is not flat, adjust the position of the blade of the fiber cleaver or replace it.

- Insert the fiber into the ceramic fiber ferrule, and thread it through.  
**Note:** The insertion should start from the sunken end of the fiber ferrule. If resistance is felt when inserting the fiber, use a new ferrule. Make as many pairs of optical fibers as possible.
- Prepare the 5-min epoxy mixture.
- Add a drop of the epoxy with a toothpick or copper wire to the sunken end of the ferrule paired with the optical fiber (Fig. 2D, E).  
**Note:** The epoxy should not extend > 1 mm–2 mm along the fiber. Remove any excess epoxy from the sides of the ferrule. If epoxy dries on the side of the

ferrule, it will be difficult to connect the implanted fiber to the patch cable for experiments.

8. Under a stereomicroscope, adjust the fiber tip at the flat end of the ferrule with a glass coverslip to make it exactly flush with the interface of the ferrule.

**Note:** There is no need for further polishing procedures if the flat fiber tip end is flush at the interface of the flat end of the ferrule. Do not leave any exposed fiber at the flat end of the ferrule: this could lead to damage of the fiber core of the patch cable.

9. Cautiously place the adjusted fiber ferrule horizontally on a clean piece of paper.  
**Note:** Make sure there is no further movement of the optical fiber along the ferrule.
10. Wait for the epoxy to dry (~30 min).
11. Check the well-dried implantable fiber with the stereomicroscope to make sure there is no exposed fiber at the flat end of the ferrule and no dried epoxy on the side of the ferrule.
12. Store the implantable fibers in any sealed container before measuring their light transmission efficacy.

#### Measuring the Light Transmission Efficacy of Implantable Optical Fibers (30 min–60 min)

13. Turn on the laser/LED of the fiber photometry system and wait ~15 min for the light intensity to stabilize.
14. Measure the intensity of the light output through the optical patch cable using the laser power meter. Adjust the actual laser power at the tip of the patch cable to ~30  $\mu$ W.  
**Note:** The reading from the laser power meter should be multiplied by a correction coefficient (2.08 for 488 nm) to obtain the actual value of laser power.
15. Connect the implantable fiber to the patch cable with a ceramic connector.
16. Measure the intensity of the light output through the implantable fiber. Keep those implantable fibers with an actual power >25  $\mu$ W, which is ~85% transmission efficacy for 30  $\mu$ W.  
**Note:** Recycle the ceramic fiber ferrules of implantable fibers with transmission efficacy < 85% by pulling the inner optical fiber out and cleaning off the dried epoxy.

#### Viral Vector Injection and Optical Fiber Implantation (Fig. 3, 1 h–2 h)

17. Weigh each mouse prior to surgery.
18. Inject 80 mg/kg pentobarbital intraperitoneally to anesthetize the mouse.

**Note:** We also use 250 mg/kg tribromoethanol (Avertin) to anesthetize mice. Wait until the mouse shows no reflex after pinching of the tail or paw with tweezers.

19. Thaw the virus on ice.  
**Note:** AAV can be stored at temperatures up to 4 °C for at least 1 month without significant loss of titer.
20. Use the Nanoliter 2010 micro-injector to withdraw an appropriate amount of viral vector; put the Nanoliter aside for later use.  
**Note:** Withdraw 100 nL more than the actual amount of viral vector that will be injected.
21. Shave the hair over the skull and mount the mouse on a stereotaxic apparatus (Fig. 3B).  
**Note:** Pull out the tongue to avoid blocking the airway.
22. Apply erythromycin ointment to maintain eye lubrication.
23. Clean the skin over the skull with 3% H<sub>2</sub>O<sub>2</sub> and open the skin to expose the skull (Fig. 3C).
24. Gently apply 3% H<sub>2</sub>O<sub>2</sub> to the surface of the skull and remove the covering tissue. Clearly expose the bregma and lambda points.
25. Use a scalpel blade to roughen the skull; this will assist firm adhesion of the ceramic ferrule to the skull with dental cement.
26. Level the skull using the anterior-posterior tilt and medial-lateral tilt on the stereotaxic apparatus.
27. Locate the appropriate location for virus injection according to a stereotaxic atlas and drill a hole (~1 mm diameter) in the skull.  
**Note:** Do not drill through the dura mater.
28. Remove the bone debris from the hole and puncture the dura using a syringe tip (0.4 mm) without damaging the cortex.
29. Drill one more hole to implant a screw to secure the dental cement.  
**Note:** It is better to drill this hole at least 2 mm away from the hole for the optical fiber.
30. Drive the anchoring screw into the skull using a micro-screwdriver and tweezers.  
**Note:** Avoid damage to the brain. There is no need to drive the screw deeply through the skull.
31. Mount the virus-filled Nanoliter 2010 to the stereotaxic arm.
32. Move the Nanoliter 2010 to the appropriate position and lower it slowly to the target coordinates.  
**Note:** Make sure that the viral solution can flow before lowering the Nanoliter 2010 into the brain.
33. Inject the viral vector at a rate of 46 nL/min to a total volume of 200 nL–500 nL (Fig. 3D).  
**Note:** The injection speed should be no faster than 100 nL/min, which may cause damage to the brain.

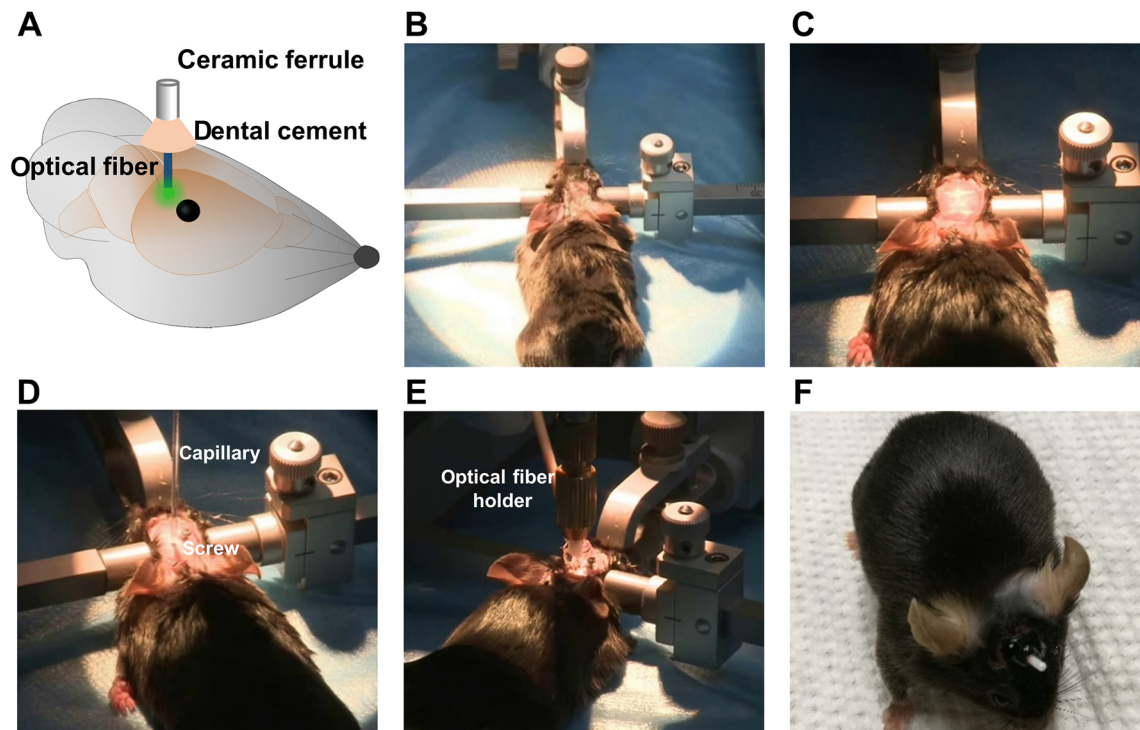


**Fig. 3** Viral vector injection and optical fiber implantation. **A** Schematic diagram of implanting optical fiber into the viral vector injection site (green color). **B** Stabilizing the anesthetized mouse in the stereotaxic apparatus. **C** Cleaning the skin on the skull and removing it to expose the skull. **D** Injecting viral vectors into the target position with Nanoliter after leveling the skull and implanting a

screw near the craniotomy for viral vector injection. **E** Inserting the implantable optical fiber into the target brain region and applying the dental cement around the ceramic ferrule to fix it on the skull. **F** Photograph of a mouse recovered from viral vector injection and optical fiber implantation surgery.

Saline should be applied to keep the exposed brain tissue in a good state.

34. After completing the injection, leave the pipette in place for 5–10 additional minutes to enable the complete diffusion of the viral solution, and then slowly withdraw it completely.
35. Attach the stereotaxic adaptor for implantable fibers to the stereotaxic arm. Insert the fiber into the stereotaxic adaptor.
- Note:** To adapt the implantable fiber to the stereotaxic adaptor, we fixed a ceramic fiber ferrule connector to the stereotaxic adaptor.
36. Lower the stereotaxic arm with the implantable fiber slowly to the brain region of interest.
37. Remove all of the remaining saline from the skull and wait it to dry completely.
38. Apply a thin layer of dental cement to the skull.
39. Apply the dental cement around the implantable optical fiber. Leave at least 4–5 mm of the ferrule of the fiber exposed (*i.e.*, not covered by headcap cement) to ensure that the fiber can be interfaced with the patch cable (Fig. 3E, F).

**Note:** Do not let the dental cement come into contact

with the skin; this will lead to unsuccessful fixation of the implanted fiber.

40. Wait until the dental cement dries completely (~30 min).
41. Remove the stereotaxic adapter from the implanted optical fiber by gently unscrewing it.
42. Apply matte black nail polish evenly to the dried dental cement to block interference from natural light during fiber photometry recording.
43. Apply lincomycin hydrochloride and lidocaine hydrochloride gel to the sterilized incision site as an analgesic and anti-inflammatory.
44. Place the mouse into a clean cage and keep it warm until it fully recovers from anesthesia.
45. House the animals individually or in groups before experiments.
- Note:** For individually-housed animals, the fiber can be protected by placing a fiber protector over the ferrule. It is also acceptable not to use a protector. Administer post-surgical analgesics as necessary.
46. Wait 10–20 days for the viral vector to initiate transgene expression and to allow the animal to fully recover. During this period, acclimate the animal by catching and holding it in the hand. With this

acclimation, animals will be habituated to having restrained movement in the experimenter's hand; this will make it easier to later connect the implanted fiber to the fiber photometry system.

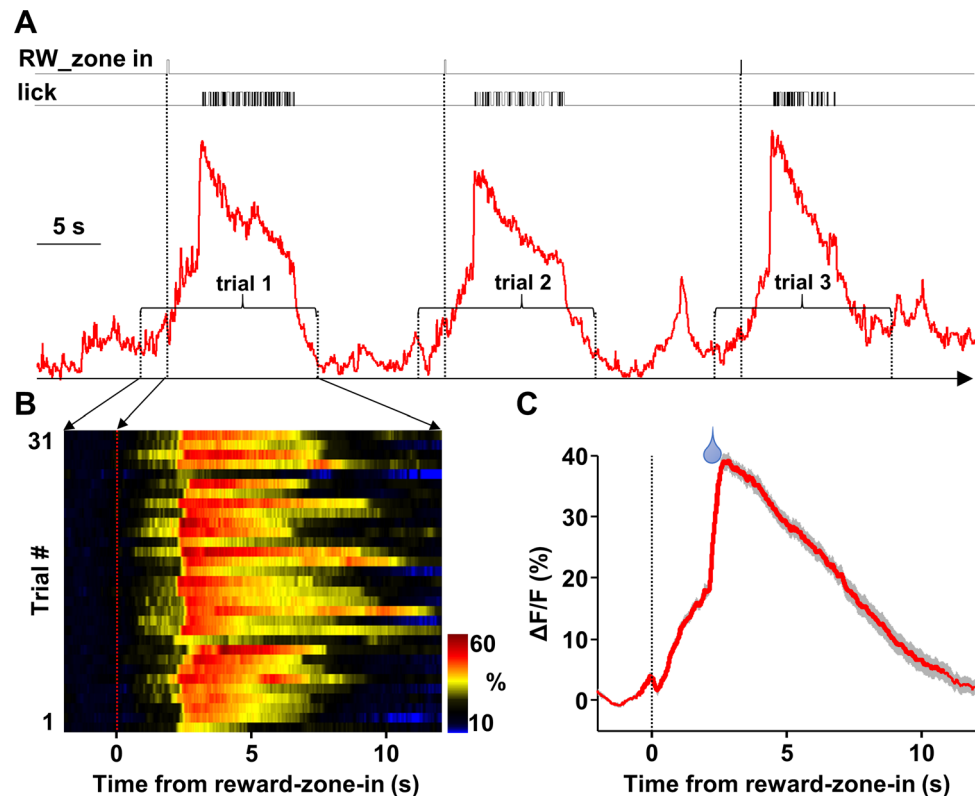
### Fiber Photometry Recording (~1 h)

47. Transport the recovered mouse to the experimental room. Habituate the mouse to the environment for 30 min.  
**Note:** Turn all the environmental lights off; make the room used for fiber photometry recording as dark as possible.
48. Turn on the fiber photometry system and the connected computer.
49. Turn on the laser/LED of the fiber photometry system and wait ~15 min for the light intensity to stabilize.
50. Check the light spot from the optical patch cable on the floor. A light spot without any black holes in it indicates that the state of the optical system is good.  
**Note:** Replace the optical patch cable of the fiber photometry system if the light spot is not in a good state. Newly-replaced optical patch cables should be bleached at a high light intensity (*e.g.*, 10 mW) for at least 20 min. Cover the ceramic connector with black heat-shrink tubing.
51. Measure the intensity of the light output through the optical patch cable using the laser power meter. Adjust the actual laser power at the tip of the patch cable to 30  $\mu$ W. Avoid using higher power, as it will lead to strong bleaching of the fluorescence signal.  
**Note:** The reading of the laser power meter should be multiplied by a correction coefficient (2.08 for 488 nm) to calculate the actual laser power value.
52. Run the software for collecting the fiber photometry data during experiments.
53. Adjust the gain of the system to an appropriate level. Do not re-adjust the gain once a single experimental session has begun.  
**Note:** We usually adjust the gain to a position with 2 V–3 V output voltage. If the signal amplitude reaches 10.5 V (the saturation level after connecting the system to the animal), adjust the gain to a lower level to obtain readings that are in-range.
54. Start recording.
55. Put a black piece of paper at the tip of the optical fiber cable and record at least 10 s as baseline before connecting to the animal.  
**Note:** The baseline value here indicates the system's offset, which should be subtracted prior to any further data analysis.
56. Catch and hold the animal. Stabilize its head between thumb and index finger.  
**Note:** Brief anesthesia with isoflurane is also acceptable. Make sure the animal recovers completely from anesthesia before conducting experiments.
57. Clean the ceramic ferrule with a cotton swab.  
**Note:** 75% ethanol or pure water is acceptable. Do not use saline.
58. Connect the implanted fiber ferrule on the animal's skull with the optical patch cable of the fiber photometry system.  
**Note:** Screw the ceramic connector down to the bottom. Hold the head of the animal firmly to facilitate screwing on the connector.
59. Release the animal, let it explore the environment freely (in a cage), and wait at least 10 min for the recorded fluorescence data to stabilize before introducing the animal to the experimental task.  
**Note:** Observe the recorded signal to see if the animal has a significant fluorescent signal. Generally, there will be a huge increase of the voltage amplitude if there is a fluorescence signal around the tip of the implanted optical fiber. The fluorescence signal amplitude will decrease quickly due to bleaching of fluorescence in the first few minutes after connecting the animal. The signal will be relative steady at a level that is still higher than the initial baseline (*i.e.*, unconnected animal). If the recorded signal does decrease, but there are no significant fluctuations in the amplitude, then abandon this experiment, because the signal in such animals does not result from virus expression. We chose 5 standard deviations from the baseline as the threshold to define a significant fluctuation in the fluorescence signal.
60. Record the fiber photometry data and animal behavior simultaneously (Fig. 4A).  
**Note:** There are two ways to store behavioral data. One is to translate behavioral events into TTL signals and record them. The other is to record the behavior as a movie, and manually find the start and end times of the behavior of interest; these time points are needed for calculation of the correlation of neuronal activity with behavior.
61. Stop recording fiber photometry data in the software when the experiment is finished.
62. Catch and hold the animal. Gently unscrew the ceramic connector and put the animal back into its home cage.

### Analysis of Event-related Fiber Photometry Data (30 min)

63. Find the start and end points of the behavior of interest, described here as events (Fig. 4A).

**Fig. 4** Analysis of event-related fiber photometry data. **A** Example raw data with calcium signal and behavior event. Segmentation of  $\text{Ca}^{2+}$  signals 2 s prior to and 12 s after reward-zone-in event. **B** Heatmap illustration of  $\text{Ca}^{2+}$  signals aligned to the initiation of reward-zone-in event. Each row plots one bout and a total of 31 bouts are illustrated. Color scale at the right indicates  $\Delta\text{F}/\text{F}$ . **C** The peri-event plot of the average  $\text{Ca}^{2+}$  transients. Thick lines indicate mean and shaded areas indicate SEM. (adapted from data published in Li *et al.* Nature Communications 2016).



64. Preprocess the fluorescence signal amplitude data with a short decay at the beginning of the recording. Fit the decay with a decreasing exponential of the form  $a \times e^{bx} + c$ , where  $a > 0$  and  $b < 0$ . Subtract the exponential fit ( $a \times e^{bx}$ ) from the original fluorescence signal amplitude. Then, subtract the baseline value that represents the system offset before further processing.
65. Calculate the fluorescence change ( $d\text{F}/\text{F}$ ) using  $(\text{F} - \text{F}_0)/\text{F}_0$  for each time point, where  $\text{F}_0$  is the processed median fluorescence value of the whole session and  $\text{F}$  represents the processed fluorescence value at each time point.
66. Find  $d\text{F}/\text{F}$  values for the behavioral events. If there are repetitive behavioral events, find all the  $d\text{F}/\text{F}$  values in a trial-by-trial manner.
67. Present the data as heat-maps (Fig. 4B) and/or peri-event plots (Fig. 4C).

## Discussion

Through the implantation of optical fibers into the brain, long-term and repetitive fiber photometry recording of neuronal activity in the same population of neurons is achievable. We have carried out fiber photometry recording from serotonin neurons in the dorsal raphe nucleus,

dopamine neurons in the ventral tegmental area, and glutamate neurons in the lateral habenula over the course of 6 days, to investigate the learning of an association between a cue and a paired reward [11, 12]. After learning, the animals were also engaged in several other behavioral sessions with fiber photometry recording. The duration of the fluorescence signal depends on the number of neurons around the distal end of the implanted optical fiber. For dopamine neurons in the ventral tegmental area, the fluorescence signal lasted  $\sim 20$  days in many animals.

It should be noted that cellular resolution is a limitation of fiber photometry recording systems. To overcome this limitation, miniature fluorescent microscopes using gradient refractive index (GRIN) lenses are a good choice. Many groups have achieved fluorescence imaging from cells in the deep brain with GRIN lenses [24–26]. These imaging setups tend to be much more expensive than fiber photometry systems, and the surgical preparation required for GRIN lens recording is much more difficult. In addition, GRIN lenses have a larger diameter (usually  $> 500 \mu\text{m}$ ), which certainly causes more damage to the brain than a  $200\text{-}\mu\text{m}$  optical fiber. Like all experimental systems, fiber photometry has advantages and disadvantages for neuroscience studies. Nevertheless, the unique advantages, including its ease of use, resistance to most electrical interference, highly efficient data collection, stability for long-term monitoring, and relatively low cost,

collectively make fiber photometry a pragmatic and often highly informative choice for neuroscience research.

**Acknowledgements** We thank J. Snyder for commenting on and editing the manuscript. We thank J. Zeng in Minmin Luo's lab for his comments. This work was supported by the Ministry of Science and Technology of China (2012YQ03026005, 2013ZX0950910, and 2015BAI08B02), the National Natural Science Foundation of China (91432114, 91632302), and the Beijing Municipal Government.

**Conflict of interest** Minmin Luo is the founder of Thinker Tech Nanjing Biotech Limited Company.

## References

- Cui G, Jun SB, Jin X, Pham MD, Vogel SS, Lovinger DM, *et al.* Concurrent activation of striatal direct and indirect pathways during action initiation. *Nature* 2013, 494: 238–242.
- Cui G, Jun SB, Jin X, Luo G, Pham MD, Lovinger DM, *et al.* Deep brain optical measurements of cell type-specific neural activity in behaving mice. *Nat Protoc* 2014, 9: 1213–1228.
- Gunaydin LA, Grosenick L, Finkelstein JC, Kauvar IV, Fenno LE, Adhikari A, *et al.* Natural neural projection dynamics underlying social behavior. *Cell* 2014, 157: 1535–1551.
- Chen Y, Lin YC, Kuo TW, Knight ZA. Sensory detection of food rapidly modulates arcuate feeding circuits. *Cell* 2015, 160: 829–841.
- Lerner TN, Shilyansky C, Davidson TJ, Evans KE, Beier KT, Zalocusky KA, *et al.* Intact-brain analyses reveal distinct information carried by SNc dopamine subcircuits. *Cell* 2015, 162: 635–647.
- Wang L, Chen IZ, Lin D. Collateral pathways from the ventromedial hypothalamus mediate defensive behaviors. *Neuron* 2015, 85: 1344–1358.
- Eban-Rothschild A, Rothschild G, Giardino WJ, Jones JR, de Lecea L. VTA dopaminergic neurons regulate ethologically relevant sleep-wake behaviors. *Nat Neurosci* 2016, 19: 1356–1366.
- Falkner AL, Grosenick L, Davidson TJ, Deisseroth K, Lin D. Hypothalamic control of male aggression-seeking behavior. *Nat Neurosci* 2016, 19: 596–604.
- Li Y, Zhong W, Wang D, Feng Q, Liu Z, Zhou J, *et al.* Serotonin neurons in the dorsal raphe nucleus encode reward signals. *Nat Commun* 2016, 7: 10503.
- Cho JR, Treweek JB, Robinson JE, Xiao C, Bremner LR, Greenbaum A, *et al.* Dorsal raphe dopamine neurons modulate arousal and promote wakefulness by salient stimuli. *Neuron* 2017, 94: 1205–1219 e1208.
- Wang D, Li Y, Feng Q, Guo Q, Zhou J, Luo M. Learning shapes the aversion and reward responses of lateral habenula neurons. *Elife* 2017, 6: e23045
- Zhong W, Li Y, Feng Q, Luo M. Learning and stress shape the reward response patterns of serotonin neurons. *J Neurosci* 2017, 37: 8863–8875.
- Li Y, Zeng J, Zhang J, Yue C, Zhong W, Liu Z, *et al.* Hypothalamic circuits for predation and evasion. *Neuron* 2018, 97: 911–924 e915.
- Mei L, Fan Y, Lv X, Welsh DK, Zhan C, Zhang EE. Long-term *in vivo* recording of circadian rhythms in brains of freely moving mice. *Proc Natl Acad Sci U S A* 2018, 115: 4276–4281.
- Liu Z, Zhou J, Li Y, Hu F, Lu Y, Ma M, *et al.* Dorsal raphe neurons signal reward through 5-HT and glutamate. *Neuron* 2014, 81: 1360–1374.
- Anikeeva P, Andalman AS, Witten I, Warden M, Goshen I, Grosenick L, *et al.* Optetrode: a multichannel readout for optogenetic control in freely moving mice. *Nat Neurosci* 2011, 15: 163–170.
- Zhou J, Jia C, Feng Q, Bao J, Luo M. Prospective coding of dorsal raphe reward signals by the orbitofrontal cortex. *J Neurosci* 2015, 35: 2717–2730.
- Chen TW, Wardill TJ, Sun Y, Pulver SR, Renninger SL, Baohan A, *et al.* Ultrasensitive fluorescent proteins for imaging neuronal activity. *Nature* 2013, 499: 295–300.
- Zhang F, Gradinaru V, Adamantidis AR, Durand R, Airan RD, de Lecea L, *et al.* Optogenetic interrogation of neural circuits: technology for probing mammalian brain structures. *Nat Protoc* 2010, 5: 439–456.
- Sparta DR, Stamatakis AM, Phillips JL, Hovelso N, van Zessen R, Stuber GD. Construction of implantable optical fibers for long-term optogenetic manipulation of neural circuits. *Nat Protoc* 2011, 7: 12–23.
- Guo Q, Zhou J, Feng Q, Lin R, Gong H, Luo Q, *et al.* Multi-channel fiber photometry for population neuronal activity recording. *Biomed Opt Express* 2015, 6: 3919–3931.
- Meng C, Zhou J, Papaneri A, Peddada T, Xu K, Cui G. Spectrally resolved fiber photometry for multi-component analysis of brain circuits. *Neuron* 2018, 98: 707–717 e704.
- Kim CK, Yang SJ, Pichamoorthy N, Young NP, Kauvar I, Jennings JH, *et al.* Simultaneous fast measurement of circuit dynamics at multiple sites across the mammalian brain. *Nat Methods* 2016, 13: 325–328.
- Ghosh KK, Burns LD, Cocker ED, Nimmerjahn A, Ziv Y, Gamal AE, *et al.* Miniaturized integration of a fluorescence microscope. *Nat Methods* 2011, 8: 871–878.
- Betley JN, Xu S, Cao ZFH, Gong R, Magnus CJ, Yu Y, *et al.* Neurons for hunger and thirst transmit a negative-valence teaching signal. *Nature* 2015, 521: 180–185.
- Jennings JH, Ung RL, Resendez SL, Stamatakis AM, Taylor JG, Huang J, *et al.* Visualizing hypothalamic network dynamics for appetitive and consummatory behaviors. *Cell* 2015, 160: 516–527.